BIOMOLECULES & THERAPEUTICS

**Original Article**
*Biomol Ther 30(4), 348-359 (2022)*

# Benzyl Isothiocyanate-Induced Cytotoxicity via the Inhibition of Autophagy and Lysosomal Function in AGS Cells

**Wah Wah Po[1,†], Won Seok Choi[1,†], Tin Myo Khing[1], Ji-Yun Lee[1], Jong Hyuk Lee[1], Joon Seok Bang[2], Young Sil Min[3], Ji Hoon Jeong[4,*] and Uy Dong Sohn[1,*]**

*[1]College of Pharmacy, Chung-Ang University, Seoul 06974,*
*[2]College of Pharmacy, Sookmyung Women's University, Seoul 04310,*
*[3]Department of Pharmaceutical Science, Jungwon University, Goesan 28024,*
*[4]College of Medicine, Chung-Ang University, and Department of Global Innovative Drugs, Graduate School of Chung-Ang University, Seoul 06974, Republic of Korea*

## Abstract

Gastric adenocarcinoma is among the top causes of cancer-related death and is one of the most commonly diagnosed carcinomas worldwide. Benzyl isothiocyanate (BITC) has been reported to inhibit the gastric cancer metastasis. In our previous study, BITC induced apoptosis in AGS cells. The purpose of the present study was to investigate the effect of BITC on autophagy mechanism in AGS cells. First, the AGS cells were treated with 5, 10, or 15 μM BITC for 24 h, followed by an analysis of the autophagy mechanism. The expression level of autophagy proteins involved in different steps of autophagy, such as LC3B, p62/SQSTM1, Atg5-Atg12, Beclin1, p-mTOR/mTOR ratio, and class III PI3K was measured in the BITC-treated cells. Lysosomal function was investigated using cathepsin activity and Bafilomycin A1, an autophagy degradation stage inhibitor. Methods including qPCR, western blotting, and immunocytochemistry were employed to detect the protein expression levels. Acridine orange staining and omnicathepsin assay were conducted to analyze the lysosomal function. siRNA transfection was performed to knock down the LC3B gene. BITC reduced the level of autophagy protein such as Beclin 1, class III PI3K, and Atg5-Atg12. BITC also induced lysosomal dysfunction which was shown as reducing cathepsin activity, protein level of cathepsin, and enlargement of acidic vesicle. Overall, the results showed that the BITC-induced AGS cell death mechanism also comprises the inhibition of the cytoprotective autophagy at both initiation and degradation steps.

**Key Words:** Benzyl isothiocyanate, AGS cell, Apoptosis, Autophagy, Lysosomal dysfunction

## INTRODUCTION

Gastric adenocarcinoma is a cancer originating from glandular epithelium of the gastric mucosa and accounts for approximately 90-95% of total gastric cancer incidence (Smyth *et al*., 2020). Given the oligosymptomatic course of early stage of gastric cancer, about two-thirds of the patients are diagnosed as advanced stage, which can only be treated with chemo or radiotherapy (Zhao *et al*., 2017). Moreover, the curative potential of the current standard treatment continues to be unsatisfactory, despite the existence of multimodal therapeutic approaches (Stock and Otto, 2005). Drug resistance is still a common problem for gastric cancer treatment, and there is a huge demand to discover and explore a new therapeutic approach or novel drug.

Recent studies showed that targeting autophagy is a promising approach for chemotherapy (Dalby *et al*., 2010; Steeves *et al*., 2010; Fulda, 2018; Amaravadi *et al*., 2019; Acevo-Rodríguez *et al*., 2020). It is a multi-step mechanism, generally divided into five; (1) initiation, (2) elongation, (3) closure, (4) fusion and (5) degradation, orchestrated by a variety of autophagy related proteins. This process is essentially a cellular recycling program. Dysfunctional or damaged cellular components are sequestered by double-membraned vesicles called autophagosomes and brought into the lumen of lysosomes, where they are broken down into basic components such as amino

**Open Access** **https://doi.org/10.4062/biomolther.2022.019**

This is an Open Access article distributed under the terms of the Creative Commons Attribution Non-Commercial License (http://creativecommons.org/licenses/by-nc/4.0/) which permits unrestricted non-commercial use, distribution, and reproduction in any medium, provided the original work is properly cited.

**Received** Feb 5, 2022 **Revised** Apr 20, 2022 **Accepted** Apr 25, 2022
**Published Online** Jul 1, 2022

***Corresponding Authors**
E-mail: udsohn@cau.ac.kr (Sohn UD), jhjeong3@cau.ac.kr (Jeong JH)
Tel: +82-2-820-5614 (Sohn UD), +82-2-820-5688 (Jeong JH)
[†]The first two authors contributed equally to this work.

Copyright © 2022 The Korean Society of Applied Pharmacology

acids that can be returned to the cytosol and reused in order to keep the cells alive (Parzych and Klionsky, 2014; Yim and Mizushima, 2020).

Studies have reported that autophagy is involved in the regulatory process of cancer cells (Feng *et al*., 2014; Amaravadi *et al*., 2019). Cancer cells grow through constant stress conditions within the tumor microenvironment. Once an anti-cancer therapy is applied, it amplifies the stress signaling in cancer cells, which then activate autophagy (Amaravadi *et al*., 2019). Depending on the level of stress conditions, autophagy in cancer cells has a dual nature as either tumor suppressing signal or tumor promoting signal (Singh *et al*., 2018). Some studies have reported that the cytoprotective function of autophagy enables tumor cell survival, which can facilitate tumor progression and confer resistance to anticancer treatments (Guo *et al*., 2013; Li *et al*., 2017, 2019). Some studies have demonstrated that certain chemotherapy or molecularly targeted therapeutics can lead to the autophagic death of cancer cells (Mathew *et al*., 2007; Wong *et al*., 2017; Law *et al*., 2019). Accordingly, cytoprotective autophagy in cancers has become a key potential target for anti-cancer therapy, and the induction of excessive or sustained autophagy has been considered as an alternative strategy for eliminating tumors (Steeves *et al*., 2010; Claerhout *et al*., 2011).

Benzyl isothiocyanate (BITC) is an isothiocyanate compound found in plants of the mustard family, including mustard, radish, broccoli, cabbage, water cress, etc. (Moy *et al*., 2009; Singh and Singh, 2012). BITC was known to have a variety of pharmacological effects. BITC has anti-inflammatory effect through suppression of NF-κB, ERK 1/2, and Akt (Lee *et al*., 2009). BITC also reduced hyperglycemia by regulating oxidative stress and GLUT4 (Chuang *et al*., 2020). BITC was shown to have a broad-spectrum antibacterial effect (Li *et al*., 2021). BITC is also well known to have anticancer activity (Dinh *et al*., 2021). Among them, research over the past decade has provided extensive evidence for the efficacy of BITC against cancer. Several studies has described the anti-cancer effects of BITC in a variety of cancer cells, including the inhibition of metastasis in colon cancer (Lai *et al*., 2010), promoting apoptosis in oral cancer (Yeh *et al*., 2016), inhibition of PI3K/AKT/FOXO pathway in pancreatic cancer (Boreddy *et al*., 2011), inducing apoptosis and cell cycle arrest in brain cancer (Zhu *et al*., 2013; Tang *et al*., 2016; Ma *et al*., 2018), inhibition of metastasis in melanoma (Lai *et al*., 2017) and more. In addition to its apoptotic, cell cycle arrest and anti-metastatic properties, BITC also influences the autophagy mechanism. In lung cancer cells and prostate cancer cells, it was reported that BITC induced the cytoprotective autophagy, but in breast cancer cell line, BITC induced autophagic cell death (Xiao *et al*., 2012; Lin *et al*., 2013; Zhang *et al*., 2017). The role of autophagy induced by BITC varies depending on the type and condition of cancer cells.

As in other cancers, BITC also has a chemotherapeutic effect on gastric cancer. Clinical evidence from China has demonstrated that isothiocyanates can protect against gastric cancer (Moy *et al*., 2009). BITC demonstrated its ability to inhibit the migration and invasion of human gastric adenocarcinoma AGS cells by suppressing ERK pathways (Ho *et al*., 2011). In our previous study, BITC induced apoptosis in AGS cells via reactive oxygen species-initiated mitochondrial dysfunction and DR4 and DR5 death receptor activation (Han *et al*., 2019). We hypothesized that BITC may also impact the autophagy mechanism of the AGS cells in addition to its apoptotic effect. Therefore, the present study was conducted to investigate the effect of BITC on the autophagy mechanism in AGS cells.

## MATERIALS AND METHODS

### Materials and reagents

All of the basic cell culture reagents were purchased from Invitrogen (Grand Island, NY, USA), Corning Inc. (NY, USA), and Welgene Inc (Daegu, Korea). To prepare the cellular extracts, RIPA lysis and extraction buffer were purchased from Thermofisher Scientific (Waltham, MA, USA), and protease and phosphatase inhibitors were purchased from Sigma Chemical Co (St. Louis, MO, USA). For cell viability assay, 3-[4,5-dimethylthiazol-2-yl]-2,5-diphenyl-tetrazolium bromide (MTT) and dimethyl sulfoxide (DMSO) were also purchased from Sigma Chemical Co. Antibodies against LC3B, Atg5, BECLIN1, p62/SQSTM1, PI3K class III, mTOR, p-mTOR, cathepsin B, and cathepsin D antibodies were purchased from Cell Signaling Technology (Danvers, MA, USA). Anti-cathepsin L, anti-LAMP2, anti-GAPDH, and anti-actin antibody were purchased from Santa Cruz Biotechnology (Santa Cruz, CA, USA). Goat anti-rabbit IgG-HRP and goat anti-mouse IgG-HRP antibodies were purchased from Bethyl Laboratories (Montgomery, TX, USA). Anti-rabbit IgG (H+L), F(ab')2 fragment (Alexa Fluor® 488 conjugate), normal goat serum, LC3B siRNA II, and control siRNA were purchased from Cell Signaling Technology. Lipofactamine RNAiMAX reagent and Opti-MEM reduced serum medium were purchased from Thermofisher Scientific. All western blotting reagents were purchased from ELPIS-BIOTECH (Daejeon, Korea) and Bio-Rad (Hercules, CA, USA). PVDF membranes were purchased from Koma Biotech (Seoul, Korea) and NC membranes were purchased from Bio-Rad. X-ray films were purchased from Thermofisher Scientific. PCR primers for hLC3B, hSQSM1 and β-actin were purchased from BIONEER (Daejeon, Korea). Nucleozol reagent was purchased from MACHEREY-NAGEL (Düren, North Rhine-Westphalia, Germany). The ReverTra Ace qPCR RT Master Mix kit was purchased from TOYOBO (Osaka, Japan), and the iQ™ SYBR® Green Supermix was obtained from Bio-Rad. Benzyl isothiocyanate (BITC), a pan-caspase inhibitor, Z-VAD-FMK, and the PI3K inhibitor, wortmannin were purchased from Selleckchem (Houston, TX, USA). Bafilomycin A1 was purchased from TOCRIS Bioscience (Bristol, UK). Omnicathepsin fluorogenic substrate (Z-FR-AMC) was purchased from ENZO Life Sciences (Farmingdale, NY, USA). 4'-6-Diamidine-2'-phenylindole dihydrochloride (DAPI) was purchased from Roche (Mannheim, Baden-Württemberg, Germany) and acridine orange (AO) was purchased from Sigma Chemical Co.

### Cell culture and morphological observation

The human gastric cancer cell line, AGS (KCLB 21739), was obtained from the Korean Cell Line Bank (Seoul, Korea). The cells were cultured in RPMI-1640 medium (Welgene Inc.) containing 10% FBS and 5% antibiotics, which consisted of 1% penicillin-streptomycin and 0.1% amphotericin B. The culture was kept at 37°C in a humidified atmosphere with 5% $CO_2$ and 95% air. Cells were seeded as a monolayer in a petri dish in a 1:10 ratio of cells to total media. They were passaged every time 90% confluence was reached.

For treatment, the cells were seeded to 70-80% confluency and incubated with different concentrations of BITC (5, 10, or 15 μM) for a specified duration. The changes in cellular morphology were observed using a fluorescence microscope (Leica, Wetzlar, Germany).

### Measurement of cell viability

To determine the cell viability, an MTT assay was performed. AGS cells were plated at a density of $1\times10^5$ cells/well in 24-well plates overnight in RPMI-1640 medium supplemented with 10% FBS and 5% antibiotics. The next day, the cells were treated with different concentrations of treatment agents. When desired treatment duration (24, 48 or 72 h) was reached, the treatment medium was removed. Then, the cells were washed twice with PBS, and MTT solution (final concentration, 0.5 mg/mL) was added into each well. After incubation for 4 h at 37°C, the medium was slowly removed, and 300 μL DMSO was added to dissolve the formazan crystals. The percent cell viability was calculated based on the absorbance measured at 570 nm by using a microplate reader (Molecular Devices, Sunnyvale, CA, USA), and normalized to control.

### DAPI staining for nuclear morphology observation

To detect the changes in nuclear morphology after BITC treatment, the AGS cells were seeded on coverslips in a 24-well plate. After treatment, they were fixed with 4% paraformaldehyde for 30 min. Next, they were washed with PBS twice and stained with 300 nM DAPI solution for 5 min at room temperature. The stain solution was then removed, and the cells were washed with PBS twice. The nuclear morphological changes were observed and imaged with a fluorescent microscope (Leica).

### Western blot analysis

After treatment, the AGS cells were collected by trypsinization and lysed with cold RIPA lysis buffer. Protein quantification was conducted with a Pierce BCA protein assay kit (Pierce Biotechnology, Rockford, IL, USA). The lysates (20-40 μg) were subjected to 7.5-15% sodium dodecyl sulfate gel electrophoresis (SDS-PAGE) and transferred to PVDF or NC membranes using a Power Pac power supply (Bio-Rad). After blocking with 5% skim milk or 5% BSA for 1 h, the membranes were incubated with the designated primary antibodies overnight at 4°C in a 1:1000 dilution. Next, they were washed three times with TBST (1% Tween 20) and incubated with secondary HRP-labeled antibodies in a 1:5000 dilution to detect the expression of the proteins of interest. Protein bands were examined using an ECL reagent (Santa Cruz Biotechnology) by the Bio-Rad Universal Hood II Gel doc system or X-ray film method. Image J (NIH Image, MD, USA) was used to analyze the data.

### Quantitative PCR analysis

The total RNA of the cells was extracted using Nucleozol reagent (MACHEREY-NAGEL). For first-strand cDNA synthesis, 1 μg RNA was reverse transcribed with ReverTra Ace qPCR RT Master Mix (TOYOBO) according to the manufacturer's instructions. Next, the synthesized cDNAs were subjected to quantitative real-time PCR analysis. The sequences of the primers used in the current study were the following: hLC3B, 5'-GTG TCC GTT CAC CAA CAG GAA G-3' (reverse), and 5'-GAG AAG CAG CTT CCT GTT CTG G-3' (forward); hSQSTM1, 5'-AGT GTC CGT GTT TCA CCT TCC G -3' (reverse) and 5'-TGT GTA GCG TCT GCG AGG GAA A-3' (forward); β-actin, 5'-TAC AGG CCG GGG AGC ATC GT-3' (reverse) and 5'-CGC CAC CAG TTC GCC ATG GA-3' (forward). Real-time PCR was performed using a qPCR instrument (CFX Connect Optics Module, Bio-Rad Laboratories, Inc, CA, USA) using iQ™ SYBR® Green Supermix (Bio-Rad) according to the manufacturer's instructions. All of the samples were analyzed in duplicate. GAPDH was used as an internal control. Gene expression was calculated using the comparative threshold cycle ($2^{-\Delta\Delta CT}$) method.

### Immunocytochemistry staining

Immunocytochemistry for LC3B and LAMP2 was performed after the AGS cells were fixed with cold 100% methanol. After blocking with normal goat serum, the cells were incubated with the primary antibody overnight at 4°C followed by incubation with Alexa Fluor 488-conjugated secondary antibody for 1 h at room temperature. Then, the nuclei were stained with 300 nM of DAPI for 5 min at room temperature. The cells were observed and imaged using a fluorescent microscope (Leica) or a confocal microscope (Zeiss, Oberkochen, Germany).

### Acridine orange staining

AGS cells were seeded with a complete medium at a density of approximately $3\times10^5$ cells in each confocal dish overnight. The next day, the cells were treated with different concentrations of BITC for 24 h and washed with PBS (10%FBS) once. After 20 min staining with 1 μg/mL acridine orange dye at room temperature, the fluorescence pattern was observed within 1 h under a confocal microscope (Zeiss).

### Cathepsin activity assay

The supernatant from AGS cell lysates was incubated with omnicathepsin fluorogenic substrate (Z-FR-AMC, 100 μM) for 30 min at 37°C. The fluorescence emitted by released AMC was quantified in a plate reader (exc: 380 nm; em: 440 nm) and normalized by total protein content.

### RNA interference

AGS cells were transfected with either 50 nM siRNA against LC3B or control siRNA using lipofectamine RNAiMAX reagent according to the manufacturer's instructions. The cells were then incubated with 10 μM BITC, and further analysis was conducted.

### Statistical analysis

Data were expressed as the mean ± SEM of at least three independent experiments. Statistical differences between the groups were calculated using the Student's *t*-test. Results were considered statistically significant for $p$ values <0.05.

## RESULTS

### BITC inhibited AGS cell viability in time and concentration-dependent manners and induced apoptotic features

The cytotoxic effect of BITC in AGS cells was initially confirmed by an MTT assay. AGS cells were treated with 2.5, 5, 10, 20, or 40 μM BITC for 24 or 48 h. Then, the MTT assay was conducted to quantify the reduction in AGS cell viability.

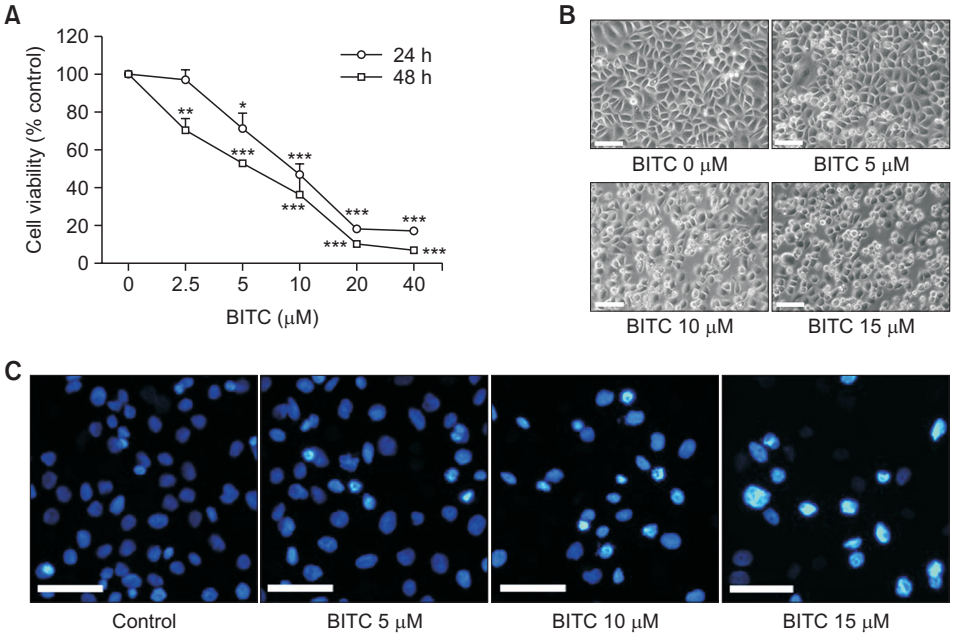


**Fig. 1.** BITC inhibited AGS cell viability in time and concentration-dependent manners and induced apoptotic features. (A) AGS cells were treated with BITC 2.5, 5, 10, 20, or 40 μM for 24 or 48 h. Then an MTT assay was conducted to measure the cell viability. (B) 6-h BITC-treated AGS cells were visualized under a fluorescence microscope to examine morphological changes (scale-bar=50 μm). (C) 24-h BITC-treated AGS cells were stained with a nuclear dye DAPI (blue) and nuclear condensation was visualized by a fluorescence microscope (scale-bar=50 μm). Data were calculated from three independent experiments and expressed as the mean ± SEM. *$p$<0.05, **$p$<0.01, and ***$p$<0.001 versus the control.

As shown in Fig. 1A, BITC reduced the AGS cell viability in time and concentration-dependent manners. The IC50 measurements for 24 h and 48 h were approximately 10 μM and 5 μM, respectively. Next, the cellular morphology was observed under a fluorescent microscope, and apoptotic features such as cell shrinkage, cell rounding, and apoptotic bodies were detected after treating the cells with BITC for 6 h (Fig. 1B). The nuclear morphological changes were also observed with a nuclear dye: DAPI under a fluorescent microscope (Fig. 1C). As a result, the number of the cells with condensed nuclei was increased significantly in a concentration-dependent manner.

### BITC increased the expression levels of LC3B and p62 proteins in AGS cells

To explore the effect of BITC on autophagy, the levels of the commonly-applied autophagy marker proteins LC3B and p62/SQSTM1 were detected by western blot and qPCR. Since autophagy is a dynamic process, the levels of both proteins were examined not only in concentration-based conditions but also in time-based conditions. As shown in Fig. 2A and 2B, BITC significantly increased the expression levels of both LC3B II and p62 in time and concentration-based conditions. BITC treatment also increased their mRNA levels (Fig. 2C). Treatment with 10 μM BITC increased the LC3B mRNA level by approximately three-fold, but this did not occur with 5 and 15 μM BITC. Treatment with 5 and 10 μM BITC increased the p62 mRNA level up to approximately three-fold, but this did not occur with 15 μM BITC.

### Effect of BITC on other autophagy markers: Beclin1 and Atg5-Atg12 protein expression and mTOR phosphorylation in AGS cells

Since autophagy is as a multi-step mechanism, the other autophagy-related proteins involved in different steps of autophagy, such as Beclin1, Atg5-Atg12 complex, and mTOR phosphorylation were analyzed by western blotting. As shown in Fig. 3, BITC decreased the expression levels of Beclin1 and Atg5-Atg12. There was a concentration-dependent decrease in Beclin1 expression. Approximately 50% and 90% of Beclin1 expression were depleted in 10 μM and 15 μM BITC-treated groups, respectively, compared to the control. For Atg5-Atg12 complex, only a high concentration 15 μM BITC significantly decreased its expression to half, compared to control group. On the other hand, statistically significant data was not obtained for mTOR phosphorylation detection.

### BITC-induced LC3B conjugation in AGS cells was not dependent on class III PI3K

The expression level of class III PI3K was measured after treating the cells with BITC for 24 h, and a potent PI3K inhibitor called wortmannin was utilized to observe the changes in LC3B conjugation level. The results showed that 15 μM BITC significantly reduced the class III PI3K protein level by approximately 50% compared to the control group (Fig. 4A). In the presence of wortmannin, the class III PI3K protein expression was significantly decreased by approximately 80%, compared to BITC monotherapy (Fig. 4A). An MTT assay was also performed to examine the cytotoxicity of wortmannin, and 24-h treatment of the typical working concentrations of wortmannin (0.2 to 1 μM) showed a 20% maximum cell death in AGS

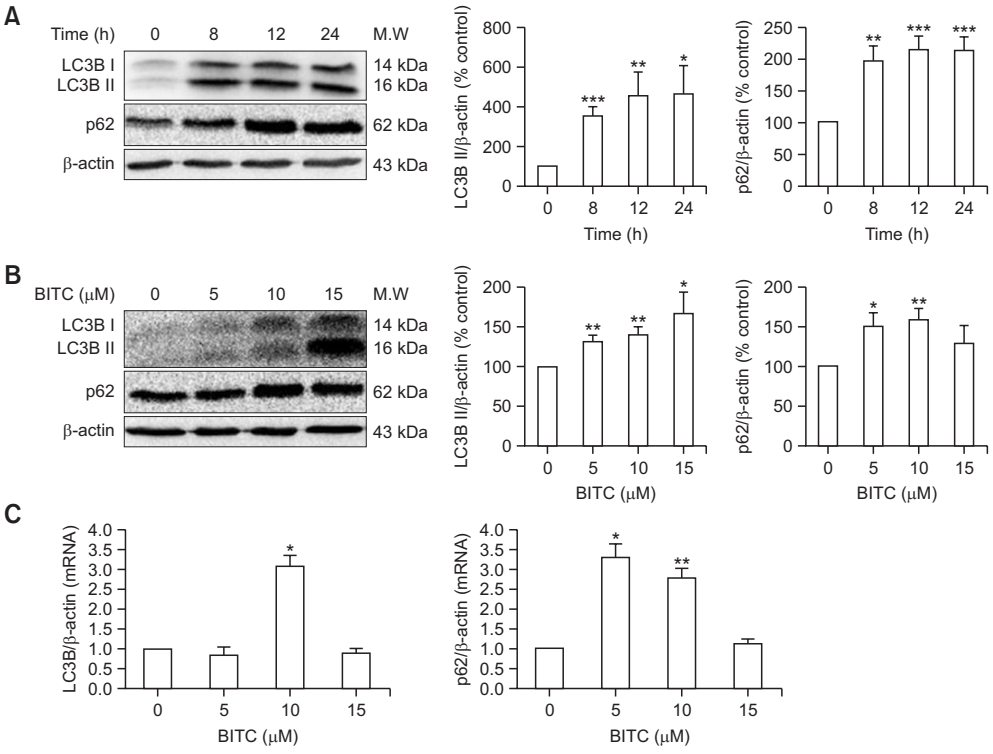


**Fig. 2.** BITC increased the expression levels of LC3B and p62 proteins AGS cells. (A) AGS cells were treated with 10 μM BITC for 8, 12, or 24 h. Whole cell lysate was prepared, and LC3B and p62 levels were determined by western blotting. β-actin was used as a loading control. (B) AGS cells were treated with 5, 10, or 15 μM BITC for 24 h. Whole cell lysate was prepared, and LC3B and p62 levels were determined by western blotting. β-actin was used as a loading control. (C) AGS cells were treated with 5, 10, or 15 μM BITC for 12 h and mRNA level was assessed by q-PCR. Data were calculated from three independent experiments and expressed as the mean ± SEM. *$p$<0.05, **$p$<0.01, and ***$p$<0.001 versus the control.

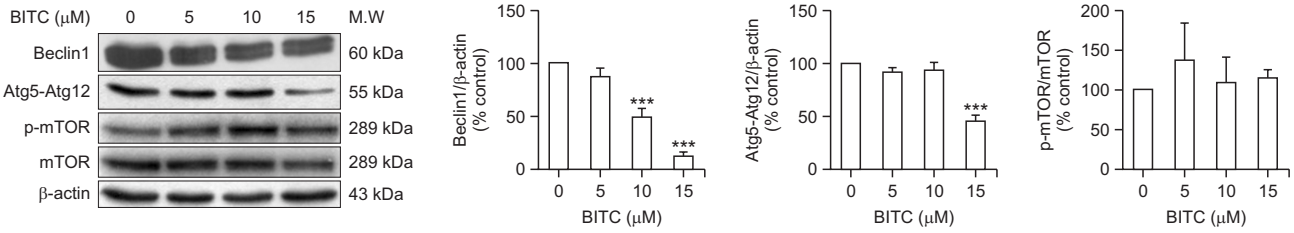


**Fig. 3.** Effect of BITC on other autophagy markers: Beclin1 and Atg5-Atg12 protein expression and mTOR phosphorylation in AGS cells. AGS cells were treated with 5, 10, or 15 μM BITC for 24 h. Whole cell lysate was prepared, and Beclin1, Atg5-Atg12, and p-mTOR/mTOR levels were determined by western blotting. β-actin was used as a loading control. Data were calculated from three independent experiments and expressed as the mean ± SEM. ***$p$<0.001 versus the control.

cells (Fig. 4B). Next, the LC3B conjugation (LC3B II level) was detected in the BITC-treated cells with or without wortmannin. As shown in Fig. 4C, wortmannin could not block the BITC-induced LC3B conjugation, and in fact, it unexpectedly enhanced the expression of LC3B II.

## BITC reduced the lysosomal cathepsin activity and caused lysosomal swelling in AGS cells

The degradation step of autophagy was investigated in AGS cells under BITC treatment. The activity of the cathepsin proteins was examined in BITC-treated AGS cells to evaluate the function of lysosomes. The cathepsin activity was quantified with an omnicathepsin assay in concentration-based or time-based conditions. As shown in Fig. 5A and 5B, BITC decreased the cathepsin activity of AGS cells in a concentration dependent manner, but not in a time-dependent manner. Bafilomycin A1 was used as a positive control to inhibit lysosomal degradation. AGS cells were treated with BITC in the presence or absence of bafilomycin A1, and the cathepsin activity was compared. As shown in Fig. 5C, bafilomycin A1 alone could reduce the basal cathepsin activity of AGS cells by approximately 60%. BITC treatment alone reduced the cathepsin activity by approximately 40% compared to the control group. In the combined treatment groups, the cathepsin

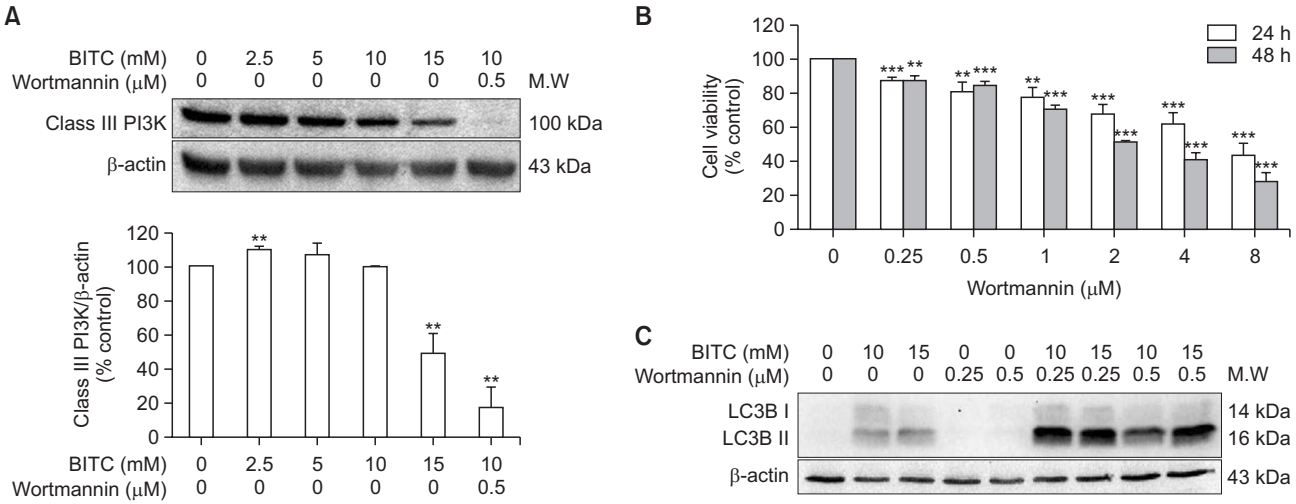


**Fig. 4.** BITC-induced LC3B conjugation in AGS cells was not dependent on class III PI3K. (A) For the single treatment, AGS cells were treated with 2.5, 5, 10, or 15 μM BITC for 24 h. For the combined treatment, the cells were pre-treated with 0.5 μM wortmannin for 2 h followed by 10 μM BITC for 24 h. Then, the whole cell lysate was prepared, and the class III PI3K protein level was measured by western blotting. β-actin was used as a loading control. (B) The cytotoxicity of wortmannin was detected by MTT assay after treating the cells with different concentrations of wortmannin for 24 and 48 h. (C) AGS cells were pre-treated with 0.25 or 0.5 μM wortmannin for 2 h followed by 10 or 15 μM BITC for 24 h. After cell lysis, the change in LC3B II level was detected by western blotting. β-actin was used as a loading control. Data were calculated from three independent experiments and expressed as the mean ± SEM. **$p$<0.01 and ***$p$<0.001 versus the control.

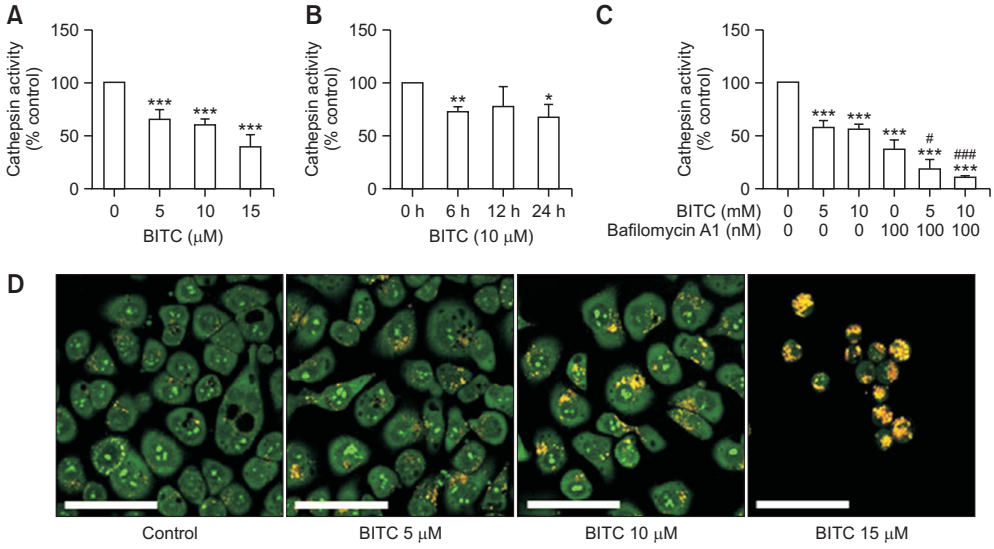


**Fig. 5.** BITC reduced the lysosomal cathepsin activity and caused lysosomal swelling in AGS cells. (A) AGS cells were treated with 5, 10, or 15 μM BITC for 24 h. Whole cell lysis was performed, and the supernatant was incubated with omnicathepsin (100 μM) for 30 min at 37°C. The emitted fluorescence was quantified in a plate reader (exc: 380 nm, em: 440 nm) and normalized by total protein concentration. (B) AGS cells were treated with 10 μM BITC for 6, 12, or 24 h. Whole cell lysis was performed, and the supernatant was incubated with omnicathepsin (100 μM) for 30 min at 37°C. The emitted fluorescence was quantified in a plate reader (exc: 380 nm, em: 440 nm) and normalized by total protein concentration. (C) AGS cells were treated with or without 100 nM bafilomycin A1 for 24 h. Whole cell lysis was performed, and the supernatant was incubated with omnicathepsin (100 μM) for 30 min at 37°C. The emitted fluorescence was quantified in a plate reader (exc: 380 nm, em: 440 nm) and normalized by total protein concentration. (D) AGS cells were treated with 5, 10, or 15 μM BITC for 24 h, stained with 1 μg/ml AO for 20 min at room temperature, and visualized by a confocal microscope within 1 h (scale-bar=50 μm). AO emits red fluorescence in the acidic compartment and green fluorescence in the cytoplasm. Data were calculated from three independent experiments and expressed as the mean ± SEM. *$p$<0.05, **$p$<0.01, ***$p$<0.001 versus the control, and $^{\#}p$<0.05, $^{\#\#\#}p$<0.001 versus BITC treatment alone.

activity significantly declined by approximately 80% or 90% compared to the control.

Next, lysosomal stability was detected via AO staining. It was predicted that BITC would decrease lysosomal stability. However, BITC did not reduce the red fluorescence or increase the green fluorescence of AO. In addition, the sizes of the red dots, which represent the acidic vesicles, were noticeably larger (Fig. 5D).

### BITC increased the expression level of lysosomal membrane protein LAMP2 in AGS cells

To confirm the lysosomal swelling, the expression level of lysosomal membrane protein LAMP2 was analyzed by western blotting and immunocytochemistry staining. Under the same conditions as the previously described experiments, AGS cells were exposed to 5, 10, or 15 μM BITC for 24 h, and the expression level of LAMP2 was measured by western blotting. For immunostaining, the cells were treated with BITC for 7 h. DAPI was used as a counterstain to stain the nuclei. The western blot analysis showed that 24-h BITC treatment significantly increased the expression level of LAMP2 in a concentration-dependent manner (Fig. 6A), whereas no difference was visualized through immunostaining in the 7-h BITC-treated cells (Fig. 6B).

### BITC reduced the quantity of mature cathepsins D, L, and B in AGS cells

To further confirm the lysosomal dysfunction induced by BITC, the expression levels of cathepsin proteins D, L, and B were measured by western blotting. As shown in Fig. 7A, after 24-h BITC treatment, pro-cathepsin D expression dramatically increased up to 4-fold. Prepro-cathepsin D expression seemed to increase slightly, but no statistically significant data was obtained. Mature-cathepsin D level was decreased by approximately 2%, 24%, and 28% after BITC treatments of 5, 10 and 15 μM, respectively, compared to the control. Similarly, 5 μM BITC increased the expression of pro-cathepsin L

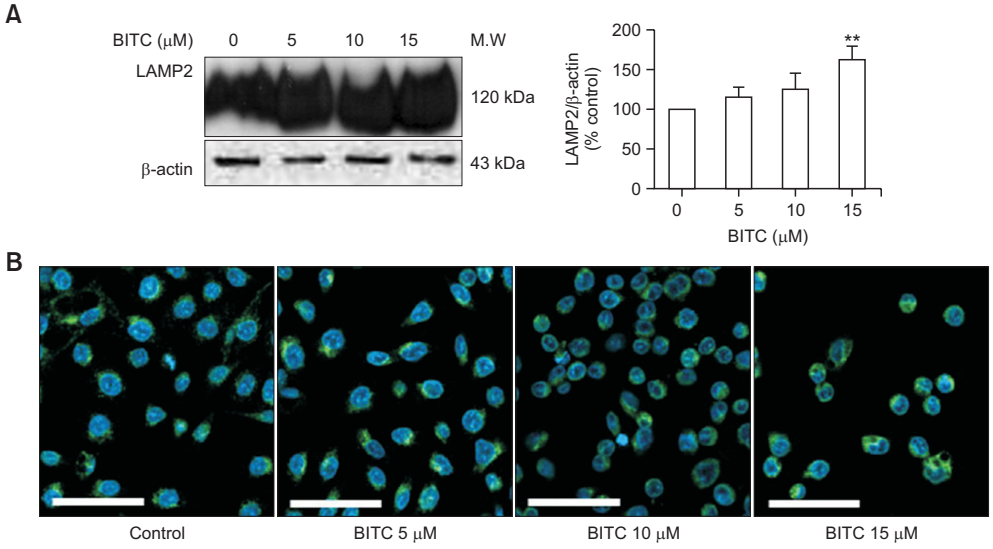


**Fig. 6.** BITC increased the expression level of lysosomal membrane protein LAMP2 in AGS cells. (A) AGS cells were treated with 5, 10, or 15 μM BITC for 24 h. Whole cell lysate was prepared, and the LAMP2 protein level was measured by western blotting. β-actin was used as a loading control. (B) AGS cells were treated with 5, 10, or 15 μM BITC for 7 h, incubated with anti-LAMP2 antibody, and was detected via Alexa Flour 488-conjugated secondary antibody (green) by a confocal microscope (scale-bar=50 μm). DAPI (blue) was used for nuclear staining. Data were calculated from three independent experiments and expressed as the mean ± SEM. ***p*<0.01 versus the control.

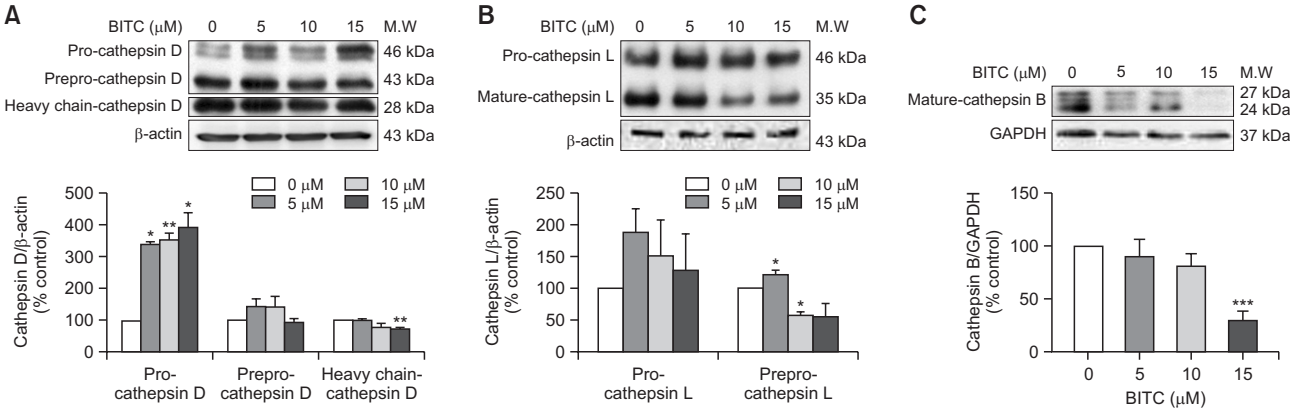


**Fig. 7.** BITC reduced the expression level of mature cathepsins D, L, and B in AGS cells. (A) AGS cells were treated with 5, 10, or 15 μM BITC for 24 h. Whole cell lysate was prepared, and the cathepsin D protein level was determined by western blotting. Under the same conditions as above, (B) cathepsin L and (C) cathepsin B protein levels were determined by western blotting. β-actin or GAPDH was used as a loading control. Data were calculated from three independent experiments and expressed as the mean ± SEM. **p*<0.05, ***p*<0.01 and ****p*<0.001 versus the control.

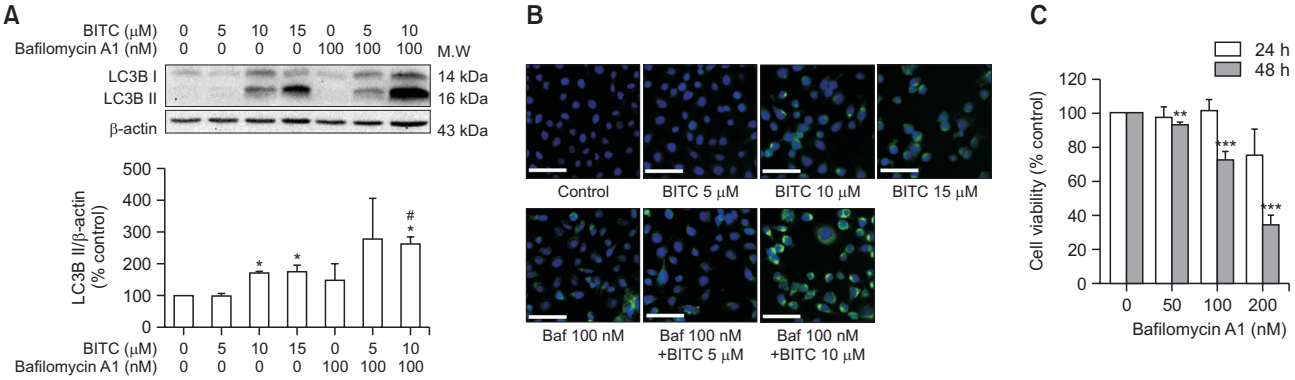


**Fig. 8.** Additive effect of BITC and bafilomycin A1 on LC3B accumulation in AGS cells. (A) AGS cells were treated with BITC with or without 100 nM bafilomycin A1 for 24 h. Whole cell lysate was prepared, and the LC3B II level was measured by western blotting. β-actin was used as a loading control. (B) Increased LC3B protein expression was further confirmed by immunostaining with anti-LC3B antibody and was detected via Alexa Flour 488-conjugated secondary antibody (green) under a fluorescence microscope (scale-bar=50 μm). DAPI (blue) was used for nuclear staining. (C) The cytotoxicity of bafilomycin A1 was investigated by MTT assay after treating the cells with different concentrations of Bafilomycin A1 for 24 and 48 h. Data were calculated from three independent experiments and expressed as the mean ± SEM. *$p$<0.05, **$p$<0.01, ***$p$<0.001 versus the control, and $^{\#}p$<0.05 versus BITC treatment alone.

to almost twice that of the control group. On the other hand, 10 and 15 μM BITC treatments reduced mature-cathepsin L expression by approximately 40% compared to the control group (Fig. 7B). As shown in Fig. 7C, BITC decreased the expression level of mature-cathepsin B by approximately 10%, 20%, and 70% in 5, 10, and 15 μM BITC-treated groups, respectively, compared to the control group.

### Additive effect of BITC and bafilomycin A1 on LC3B accumulation in AGS cells

Next, the lysosomal degradation inhibitor bafilomycin A1 was utilized, and the LC3B II accumulation pattern was assessed by western blotting and immunocytochemistry staining. As shown in Fig. 8A and 8B, the combined treatment of BITC and bafilomycin A1 showed a remarkable additive effect on LC3B II accumulation. Compared to 10 μM BITC treatment alone, LC3B II level increased by approximately 1.5 times in the presence of bafilomycin A1 in western blotting. The cytotoxicity of bafilomycin A1 was evaluated by an MTT assay, and it was confirmed that the applied concentration and duration of bafilomycin A1 treatment (100 nM, 24 h) did not induce cytotoxicity to AGS cells (Fig. 8C).

### Inhibition of different stages of autophagy and its effect on the cytotoxicity of BITC in AGS cells

After confirming the BITC-induced autophagy inhibition through lysosomal dysfunction, the role of basal autophagy in AGS cells was determined using an MTT assay. The difference in cell viability level was detected by further inhibiting autophagy with different autophagic stage inhibitors: wortmannin to inhibit autophagy initiation, and Bafilomycin A1 to block the autophagy degradation. As shown in Fig. 9A and 9B, wortmannin significantly increased BITC-induced cell death, but bafilomycin A1 did not.

### No relationship between BITC-induced LC3 B accumulation and cytotoxicity

Next, the probable relationship between BITC-induced LC3B accumulation and cell death was investigated. Specific siRNA was used to knock down the LC3B gene. The cells

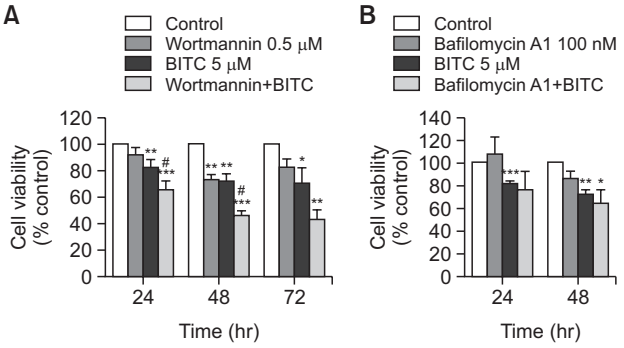


**Fig. 9.** Inhibition of different stages of autophagy and its effect on the cytotoxicity of BITC in AGS cells. AGS cells were treated with BITC for 24 h after 2-h pre-treatment with (A) 0.5 μM wortmannin and (B) 100 nM bafilomycin A1. Then, the cell viability was measured by MTT assay. Data were calculated from at least three independent experiments and expressed as the mean ± SEM. *$p$<0.05, **$p$<0.01, ***$p$<0.001 versus the control, and $^{\#}p$<0.05 versus BITC treatment alone.

were transfected with the LC3B siRNA for 12 h, followed by an 8-h BITC treatment. Transfection efficacy was confirmed by the almost depleted LC3B protein expression observed via western blotting. A control siRNA was used as a negative control (Fig. 10A). An MTT assay was continuously conducted, and the changes in cell viability in the 24-h BITC-treated cells with and without LC3B siRNA were determined. As shown in Fig. 10B, the knockdown of LC3B did not influence the cell death induced by BITC.

## DISCUSSION

BITC was known to have anticancer effect, and our previous study demonstrated that the mechanism of anticancer effect results from inducing apoptosis (Han *et al*., 2019). On the other hand, autophagy has a relationship with cancer. In this study, we focus on the tumor promoting effect of autophagy.

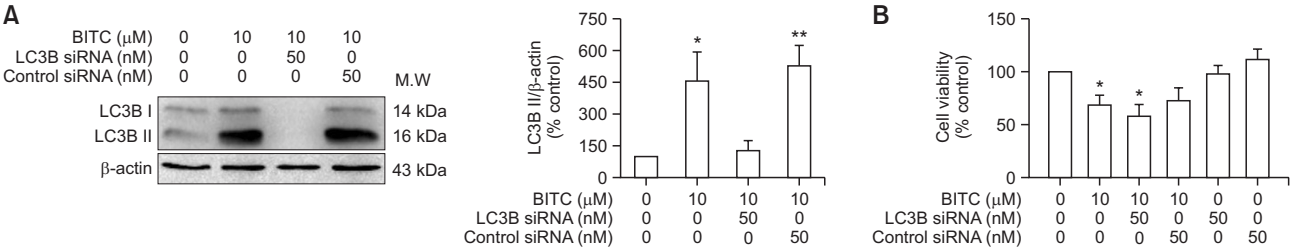


**Fig. 10.** No relationship between BITC-induced LC3 B accumulation and cytotoxicity. (A) AGS cells were transfected with 50 nM LC3B siRNA or control siRNA for 12 h and incubated with 10 μM BITC for 8 h. Whole cell lysate was prepared, and siRNA efficacy was confirmed by detecting the LC3B protein expression via western blotting. β-actin was used as a loading control. (B) AGS cells were transfected with 50 nM LC3B siRNA or control siRNA for 12 h, followed by 10 μM BITC treatment for 24 h. Cell viability changes were evaluated by MTT assay. Data were calculated from three independent experiments and expressed as the mean ± SEM. **p*<0.05, ***p*<0.01 versus the control.

Furthermore, it was reported that autophagy maintains the survival of gastric cancer cells and affects the resistance of anti-cancer drugs (Cao *et al*., 2019). Here, we showed that BITC was related to autophagy as a new anticancer mechanism of BITC.

Autophagy has a dual role in gastric cancer as either a tumor suppressor or tumor promoter, depending on the stress conditions (Cao *et al*., 2019). In the relationship between autophagy and apoptosis, autophagy often occurs in a sequence that precedes apoptosis because stress often stimulates an autophagic response (Mariño *et al*., 2014). However, there is an also inhibitory crosstalk between autophagy and apoptosis. Autophagy can reduce a possibility to undergo apoptosis (Jung *et al*., 2020). Damaged mitochondria which can activate the apoptotic programmed cell death were removed by mitophagy which is selective autophagy of mitochondria (Youle and Narendra, 2011). In addition, autophagy can also attenuate apoptosis by selectively reducing the amount of pro-apoptotic proteins in the cytoplasm (Mariño *et al*., 2014). In previous research, BITC has different effects for each cell type. BITC induces protective autophagy in lung cancer cells (Zhang *et al*., 2017), prostate cancer cells (Lin *et al*., 2013), and colon cancer cells (Liu *et al*., 2017) but BITC causes autophagic cell death in breast cancer cells (Xiao *et al*., 2012).

In our previous study, we found that BITC induced both intrinsic and extrinsic apoptosis in gastric cancer cells. In addition to apoptosis, the present study found that BITC increased the protein expression levels of both LC3B II and p62 in time and concentration-dependent manners. LC3 and p62 are well known and commonly applied autophagy markers (Mizushima *et al*., 2010). When autophagy degradation occurs, LC3 II detaches from the outer membrane while both LC3 II from inner membrane and p62 are degraded along with the cargo by lysosomal proteases (Mizushima *et al*., 2010). Some studies reported that both LC3 and p62 proteins increased while the autophagic degradation was inhibited (Pugsley, 2017; Yi *et al*., 2018). In the current study, BITC induced the accumulation of both LC3B II and p62 proteins in AGS cells, suggesting that BITC may impair autophagic degradation. On the other hand, BITC increased the mRNA levels of both LC3B and p62 in AGS cells, which suggests that the host AGS cells may generate more autophagy proteins as a response against the BITC-induced stress.

Meanwhile, BITC did not alter mTOR phosphorylation, but it significantly decreased the levels of both Beclin1 and Atg5-Atg12 proteins in AGS cells. mTOR is an upstream negative regulator of autophagy, and the inhibition of mTOR phosphorylation enhances autophagy (Dossou and Basu, 2019; Wang and Zhang, 2019). On the other hand, Beclin1 is involved in the initiation step of autophagy and is essential for autophagy (Liang *et al*., 1999). It forms a regulatory complex with class III PI3K and recruits the required proteins for autophagosome formation (Acevo-Rodríguez *et al*., 2020). The Atg5-Atg12 complex functions as a ubiquitin E3-like enzyme to convert LC3 I to LC3 II, which is required for the autophagosome membrane elongation process (Green and Llambi, 2015). Accordingly, it was assumed that the lack of effect on p-mTOR and the decreased expression levels of both Beclin1 and Atg5-Atg12 complex were due to the BITC-induced inhibition of the autophagy initiation step. Consistent with the present study, other researchers have observed autophagy inhibition through the reduction of Beclin1 and Atg5 proteins (Chen *et al*., 2018; Rubio and Mohr, 2019).

Furthermore, the results showed that 15 μM BITC decreased the class III PI3K protein expression in AGS cells. Notably, the LC3B II accumulation induced by BITC was enhanced in the presence of wortmannin, a potent PI3K inhibitor. Evidence has shown that class III PI3K is essential for LC3 conjugation (conversion of LC3 I to LC3 II) to initiate the autophagy process (Jaber and Zong, 2013; Ge *et al*., 2014; Pasquier *et al*., 2015; Brier *et al*., 2019). Thus, the decrease in class III PI3K following BITC treatment suggested that BITC decreased the autophagy initiation. Moreover, since the increased LC3B II level induced by BITC was still high in the presence of a class III PI3K inhibitor, it was assumed that BITC induced LC3B conjugation did not depend on class III PI3K. Consistent with the present study, another study reported that even in class III PI3K-null MEF cells, LC3 conjugation still occurred while autophagy degradation decreased (Jaber and Zong, 2013). Therefore, it was hypothesized that BITC-induced LC3 II accumulation in AGS cells may not act as an autophagy induction signal and may be a consequence of decreased autophagy degradation.

Lysosomes play a key role in autophagic degradation (Yim and Mizushima, 2020). In this study, BITC reduced the cathepsin activity of AGS cells in concentration and time-dependent manners. Moreover, a synergistic decrease in cathepsin activity was found in the combined treatment of BITC and bafilomycin A1, a specific inhibitor of V-ATPase that strongly inhibits the acidification of lysosomes and blocks lysosomal degradation (Yoshimori *et al*., 1991). Consistent with the results of a qualitative assay, a western blot analysis showed a significant

decrease in the quantity of active forms of cathepsin proteins D, B, and L in the BITC-treated AGS cells. These data clearly indicate that BITC reduced the function of lysosomes. In accordance with these results, other studies reported that the inhibition of cathepsin induced the lysosomal dysfunction (Jung *et al*., 2015; Cermak *et al*., 2016). In addition, the present study found that BITC increased the size of the acidic vesicles in AGS cells and upregulated a major lysosomal surface protein; LAMP2, suggesting lysosomal swelling. Enlarged lysosomes and LAMP2 upregulation are known to contribute to lysosomal dysfunction (Wang *et al*., 2018; Li *et al*., 2020).

In addition, lysosomal dysfunction is one of the reasons for the LC3 II accumulation (Rossi *et al*., 2009; Zhang *et al*., 2020). The combined treatment of BITC and bafilomycin A1 had a significant additive effect on LC3B II accumulation, which may be due to the early, synergistic reduction in cathepsin activity by both compounds. To the best of our knowledge, this is the first study on the effect of BITC specifically on lysosomal function.

Furthermore, BITC induced synergistic cell death with the PI3K inhibitor wortmannin, but not with bafilomycin A1, a lysosomal degradation inhibitor. This suggests that wortmannin and BITC may complement each other's function to inhibit autophagy by inhibiting the autophagy initiation step and degradation step, respectively. Therefore, as autophagy inhibition increases, there would be a greater quantity of dead cells if the basal autophagy in AGS cells has a pro-survival role. For bafilomycin A1, it is possible that its mechanism overlaps with BITC, and competition may have occurred. Nevertheless, the increased cell death with wortmannin indicated the tumor-promoting role of basal autophagy in AGS cells. This suggests that the BITC induced autophagy inhibition may be beneficial for gastric cancer treatment.

In this study, the relative toxicity of BITC in normal cells was not examined due to limited time and resources. However, toxicity testing of BITC in normal cells has already been conducted in several studies. In one example, BITC inhibited cell growth, promoted G2/M phase arrest, and triggered apoptosis of oral cancer OC2 cells, with a minimal toxicity to normal PBMCs (Yeh *et al*., 2016). Similarly, BITC has been found to induce apoptosis in breast cancer cells but has no effect on normal breast MCF-10A cells (Sehrawat *et al*., 2016). These studies suggested that BITC has selective toxicity to tumor cells and is safe to be used for cancer treatment.

A previous study reported on the novel role of LC3-induced non-autophagic cell death in 15d-PGJ2 treated cancer cells (Kar *et al*., 2009). Thus, the present study examined the difference in cell viability in the presence and absence of BITC-induced LC3B accumulation by knocking down the LC3B gene with siRNA. No significant difference was found in the cell viability in the presence or absence of LC3B siRNA, suggesting an indirect relationship between the BITC-induced LC3B upregulation and the cytotoxicity in AGS cells.

In summary, the BITC-induced AGS cell death mechanism involves autophagy inhibition in addition to its apoptotic effect. BITC could inhibit the cytoprotective autophagy of AGS cells by decreasing both the autophagy initiator proteins and the lysosomal degradation. The results of this study provide a basic for BITC as a novel anti-cancer agent and support autophagy as a promising target for gastric cancer treatment (Fig. 11).

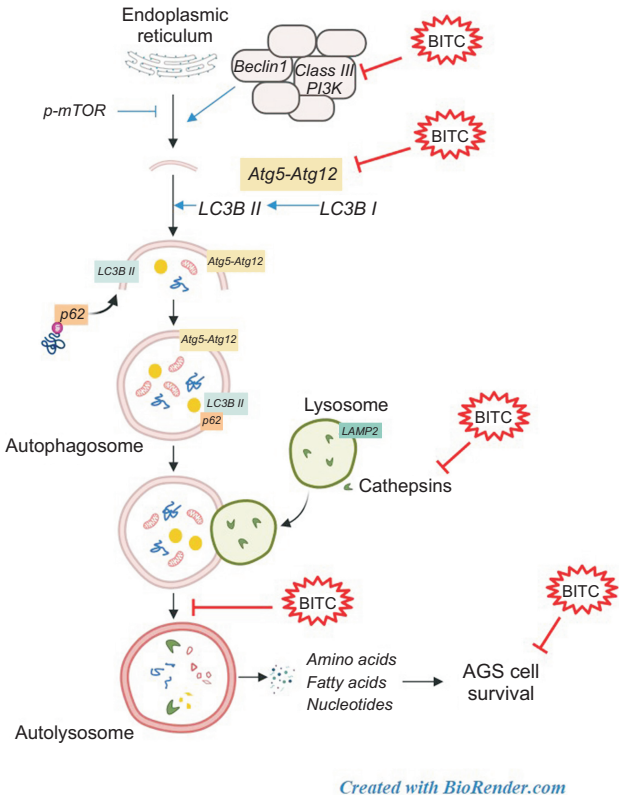


**Fig. 11.** The proposed mechanism of BITC-induced cytotoxicity through autophagy inhibition and lysosomal dysfunction in AGS cells. In human gastric adenocarcinoma AGS cells, BITC induced cell death by caspase-dependent apoptosis and inhibition of cytoprotective autophagy. It inhibited autophagy degradation through lysosomal dysfunction, which decreased both the quality and quantity of cathepsin proteins. Moreover, BITC may inhibit the autophagy initiation and elongation steps, since it decreased the expression levels of Beclin1, Atg5-Atg12 complex, and class III PI3K proteins. However, because of increased mRNA transcription and decreased lysosomal degradation, BITC also caused the accumulation of LC3B and p62. Nevertheless, there was no direct relationship between BITC-induced LC3B II accumulation and cytotoxicity.

## CONFLICT OF INTEREST

There is no conflict of interest to declare.

## ACKNOWLEDGMENTS

This research was supported by the Basic Science Research Program through the National Research Foundation of Korea (NRF), funded by the Ministry of Education, Science and Technology [Grant NRF-2019R1F1A1062070], the National Research Foundation of Korea (NRF) grant funded by the Korea government (MSIT) (No.NRF-2021R1F1A1050004), and the Chung-Ang University Young Scientist Scholarship (CAYSS) program in 2017.

## REFERENCES


Acevo-Rodríguez, P. S., Maldonado, G., Castro-Obregón, S. and Hernández, G. (2020) Autophagy regulation by the translation machinery and its implications in cancer. *Front. Oncol.* **10**, 322.

Amaravadi, R. K., Kimmelman, A. C. and Debnath, J. (2019) Targeting autophagy in cancer: recent advances and future directions. *Cancer Discov.* **9**, 1167-1181.

Boreddy, S. R., Pramanik, K. C. and Srivastava, S. K. (2011) Pancreatic tumor suppression by benzyl isothiocyanate is associated with inhibition of PI3K/AKT/FOXO pathway. *Clin. Cancer Res.* **17**, 1784-1795.

Brier, L. W., Ge, L., Stjepanovic, G., Thelen, A. M., Hurley, J. H. and Schekman, R. (2019) Regulation of LC3 lipidation by the autophagy-specific class III phosphatidylinositol-3 kinase complex. *Mol. Biol. Cell* **30**, 1098-1107.

Cao, Y., Luo, Y., Zou, J., Ouyang, J., Cai, Z., Zeng, X., Ling, H. and Zeng, T. (2019) Autophagy and its role in gastric cancer. *Clin. Chim. Acta* **489**, 10-20.

Cermak, S., Kosicek, M., Mladenovic-Djordjevic, A., Smiljanic, K., Kanazir, S. and Hecimovic, S. (2016) Loss of cathepsin B and L leads to lysosomal dysfunction, NPC-like cholesterol sequestration and accumulation of the key Alzheimer's proteins. *PLoS ONE* **11**, e0167428.

Chen, J., Zhang, L., Zhou, H., Wang, W., Luo, Y., Yang, H. and Yi, H. (2018) Inhibition of autophagy promotes cisplatin-induced apoptotic cell death through Atg5 and Beclin 1 in A549 human lung cancer cells. *Mol. Med. Rep.* **17**, 6859-6865.

Chuang, W.-T., Yen, C.-C., Huang, C.-S., Chen, H.-W. and Lii, C.-K. (2020) Benzyl isothiocyanate ameliorates high-fat diet-induced hyperglycemia by enhancing Nrf2-dependent antioxidant defense-mediated IRS-1/AKT/TBC1D1 signaling and GLUT4 expression in skeletal muscle. *J. Agric. Food Chem.* **68**, 15228-15238.

Claerhout, S., Lorenzi, P. L., Weinstein, J. N. and Mills, G. B. (2011) Modulation of autophagy and its potential for cancer therapy. *Drug Future* **36**, 919-925.

Dalby, K. N., Tekedereli, I., Lopez-Berestein, G. and Ozpolat, B. (2010) Targeting the prodeath and prosurvival functions of autophagy as novel therapeutic strategies in cancer. *Autophagy* **6**, 322-329.

Dinh, T. N., Parat, M.-O., Ong, Y. S. and Khaw, K. Y. (2021) Anticancer activities of dietary benzyl isothiocyanate: a comprehensive review. *Pharmacol. Res.* **169**, 105666.

Dossou, A. S. and Basu, A. (2019) The emerging roles of mTORC1 in macromanaging autophagy. *Cancers* **11**, 1422.

Feng, Y., He, D., Yao, Z. and Klionsky, D. J. (2014) The machinery of macroautophagy. *Cell Res.* **24**, 24-41.

Fulda, S. (2018) Targeting autophagy for the treatment of cancer. *Biol. Chem.* **399**, 673-677.

Ge, L., Zhang, M. and Schekman, R. (2014) Phosphatidylinositol 3-kinase and COPII generate LC3 lipidation vesicles from the ER-Golgi intermediate compartment. *eLife* **3**, e04135.

Green, D. R. and Llambi, F. (2015) Cell death signaling. *Cold Spring Harbor Perspect. Biol.* **7**, a006080.

Guo, J. Y., Xia, B. and White, E. (2013) Autophagy-mediated tumor promotion. *Cell* **155**, 1216-1219.

Han, K. W. W., Po, W. W., Sohn, U. D. and Kim, H.-J. (2019) Benzyl isothiocyanate induces apoptosis via reactive oxygen species-initiated mitochondrial dysfunction and DR4 and DR5 death receptor activation in gastric adenocarcinoma cells. *Biomolecules* **9**, 839.

Ho, C. C., Lai, K. C., Hsu, S. C., Kuo, C. L., Ma, C. Y., Lin, M. L., Yang, J. S. and Chung, J. G. (2011) Benzyl isothiocyanate (BITC) inhibits migration and invasion of human gastric cancer AGS cells via suppressing ERK signal pathways. *Hum. Exp. Toxicol.* **30**, 296-306.

Jaber, N. and Zong, W.-X. (2013) Class III PI3K Vps34: essential roles in autophagy, endocytosis, and heart and liver function. *Ann. N. Y. Acad. Sci.* **1280**, 48-51.

Jung, M., Lee, J., Seo, H. Y., Lim, J. S. and Kim, E. K. (2015) Cathepsin inhibition-induced lysosomal dysfunction enhances pancreatic beta-cell apoptosis in high glucose. *PLoS ONE* **10**, e0116972.

Jung, S., Jeong, H. and Yu, S.-W. (2020) Autophagy as a decisive process for cell death. *Exp. Mol. Med.* **52**, 921-930.

Kar, R., Singha, P. K., Venkatachalam, M. A. and Saikumar, P. (2009) A novel role for MAP1 LC3 in nonautophagic cytoplasmic vacuolation death of cancer cells. *Oncogene* **28**, 2556-2568.

Lai, K.-C., Huang, A.-C., Hsu, S.-C., Kuo, C.-L., Yang, J.-S., Wu, S.-H. and Chung, J.-G. (2010) Benzyl isothiocyanate (BITC) inhibits migration and invasion of human colon cancer HT29 cells by inhibiting matrix metalloproteinase-2/-9 and urokinase plasminogen (uPA) through PKC and MAPK signaling pathway. *J. Agric. Food Chem.* **58**, 2935-2942.

Lai, K. C., Hsiao, Y. T., Yang, J. L., Ma, Y. S., Huang, Y. P., Chiang, T. A. and Chung, J. G. (2017) Benzyl isothiocyanate and phenethyl isothiocyanate inhibit murine melanoma B16F10 cell migration and invasion *in vitro*. *Int. J. Oncol.* **51**, 832-840.

Law, B. Y. K., Michelangeli, F., Qu, Y. Q., Xu, S.-W., Han, Y., Mok, S. W. F., Dias, I. R. d. S. R., Javed, M.-u.-H., Chan, W.-K., Xue, W.-W., Yao, X.-J., Zeng, W., Zhang, H., Wang, J.-R., Liu, L. and Wong, V. K. W. (2019) Neferine induces autophagy-dependent cell death in apoptosis-resistant cancers via ryanodine receptor and Ca2+-dependent mechanism. *Sci. Rep.* **9**, 20034.

Lee, Y. M., Seon, M. R., Cho, H. J., Kim, J.-S. and Park, J. H. Y. (2009) Benzyl isothiocyanate exhibits anti-inflammatory effects in murine macrophages and in mouse skin. *J. Mol. Med.* **87**, 1251.

Li, I. H., Shih, J.-H., Yeh, T.-Y., Lin, H.-C., Chen, M.-H. and Huang, Y.-S. (2020) Lysosomal dysfunction and autophagy blockade contribute to MDMA-induced neurotoxicity in SH-SY5Y neuroblastoma cells. *Chem. Res. Toxicol.* **33**, 903-914.

Li, P., Zhao, Y.-m., Wang, C. and Zhu, H.-p. (2021) Antibacterial activity and main action pathway of benzyl isothiocyanate extracted from papaya seeds. *J. Food Sci.* **86**, 169-176.

Li, X., Zhou, Y., Li, Y., Yang, L., Ma, Y., Peng, X., Yang, S., Liu, J. and Li, H. (2019) Autophagy: a novel mechanism of chemoresistance in cancers. *Biomed. Pharmacother.* **119**, 109415.

Li, Y. J., Lei, Y. H., Yao, N., Wang, C. R., Hu, N., Ye, W. C., Zhang, D. M. and Chen, Z. S. (2017) Autophagy and multidrug resistance in cancer. *Chin. J. Cancer* **36**, 52.

Liang, X. H., Jackson, S., Seaman, M., Brown, K., Kempkes, B., Hibshoosh, H. and Levine, B. (1999) Induction of autophagy and inhibition of tumorigenesis by beclin 1. *Nature* **402**, 672-676.

Lin, J. F., Tsai, T. F., Liao, P. C., Lin, Y. H., Lin, Y. C., Chen, H. E., Chou, K. Y. and Hwang, T. I. (2013) Benzyl isothiocyanate induces protective autophagy in human prostate cancer cells via inhibition of mTOR signaling. *Carcinogenesis* **34**, 406-414.

Liu, X., Abe-Kanoh, N., Liu, Y., Zhu, B., Munemasa, S., Nakamura, T., Murata, Y. and Nakamura, Y. (2017) Inhibition of phosphatidylinositide 3-kinase impairs the benzyl isothiocyanate-induced accumulation of autophagic molecules and Nrf2 in human colon cancer cells. *Biosci. Biotechnol. Biochem.* **81**, 2212-2215.

Ma, Y. S., Lin, J. J., Lin, C. C., Lien, J. C., Peng, S. F., Fan, M. J., Hsu, F. T. and Chung, J. G. (2018) Benzyl isothiocyanate inhibits human brain glioblastoma multiforme GBM 8401 cell xenograft tumor in nude mice *in vivo*. *Environ. Toxicol.* **33**, 1097-1104.

Mariño, G., Niso-Santano, M., Baehrecke, E. H. and Kroemer, G. (2014) Self-consumption: the interplay of autophagy and apoptosis. *Nat. Rev. Mol. Cell Biol.* **15**, 81-94.

Mathew, R., Karantza-Wadsworth, V. and White, E. (2007) Role of autophagy in cancer. *Nat. Rev. Cancer* **7**, 961-967.

Mizushima, N., Yoshimori, T. and Levine, B. (2010) Methods in mammalian autophagy research. *Cell* **140**, 313-326.

Moy, K. A., Yuan, J. M., Chung, F. L., Wang, X. L., Van Den Berg, D., Wang, R., Gao, Y. T. and Yu, M. C. (2009) Isothiocyanates, glutathione S-transferase M1 and T1 polymorphisms and gastric cancer risk: a prospective study of men in Shanghai, China. *Int. J. Cancer* **125**, 2652-2659.

Parzych, K. R. and Klionsky, D. J. (2014) An overview of autophagy: morphology, mechanism, and regulation. *Antioxid. Redox Signal.* **20**, 460-473.

Pasquier, B., El-Ahmad, Y., Filoche-Rommé, B., Dureuil, C., Fassy, F., Abecassis, P. Y., Mathieu, M., Bertrand, T., Benard, T., Barrière, C., El Batti, S., Letallec, J. P., Sonnefraud, V., Brollo, M., Delbarre, L., Loyau, V., Pilorge, F., Bertin, L., Richepin, P., Arigon, J., Labrosse, J. R., Clément, J., Durand, F., Combet, R., Perraut, P., Leroy, V., Gay, F., Lefrançois, D., Bretin, F., Marquette, J. P., Michot, N., Caron, A., Castell, C., Schio, L., McCort, G., Goulaouic, H., Garcia-

Echeverria, C. and Ronan, B. (2015) Discovery of (2S)-8-[(3R)-3-methylmorpholin-4-yl]-1-(3-methyl-2-oxobutyl)-2-(trifluoromethyl)-3,4-dihydro-2H-pyrimido[1,2-a]pyrimidin-6-one: a novel potent and selective inhibitor of Vps34 for the treatment of solid tumors. *J. Med. Chem.* **58**, 376-400.

Pugsley, H. R. (2017) Assessing autophagic flux by measuring LC3, p62, and LAMP1 co-localization using multispectral imaging flow cytometry. *J. Vis. Exp.* **21**, 55637.

Rossi, M., Munarriz, E. R., Bartesaghi, S., Milanese, M., Dinsdale, D., Guerra-Martin, M. A., Bampton, E. T. W., Glynn, P., Bonanno, G., Knight, R. A., Nicotera, P. and Melino, G. (2009) Desmethylclomipramine induces the accumulation of autophagy markers by blocking autophagic flux. *J. Cell Sci.* **122**, 3330-3339.

Rubio, R. M. and Mohr, I. (2019) Inhibition of ULK1 and Beclin1 by an α-herpesvirus Akt-like Ser/Thr kinase limits autophagy to stimulate virus replication. *Proc. Natl. Acad. Sci. U.S.A.* **116**, 26941-26950.

Sehrawat, A., Croix, C. S., Baty, C. J., Watkins, S., Tailor, D., Singh, R. P. and Singh, S. V. (2016) Inhibition of mitochondrial fusion is an early and critical event in breast cancer cell apoptosis by dietary chemopreventative benzyl isothiocyanate. *Mitochondrion* **30**, 67-77.

Singh, S. S., Vats, S., Chia, A. Y.-Q., Tan, T. Z., Deng, S., Ong, M. S., Arfuso, F., Yap, C. T., Goh, B. C., Sethi, G., Huang, R. Y.-J., Shen, H. M., Manjithaya, R. and Kumar, A. P. (2018) Dual role of autophagy in hallmarks of cancer. *Oncogene* **37**, 1142-1158.

Singh, S. V. and Singh, K. (2012) Cancer chemoprevention with dietary isothiocyanates mature for clinical translational research. *Carcinogenesis* **33**, 1833-1842.

Smyth, E. C., Nilsson, M., Grabsch, H. I., van Grieken, N. C. T. and Lordick, F. (2020) Gastric cancer. *Lancet* **396**, 635-648.

Steeves, M. A., Dorsey, F. C. and Cleveland, J. L. (2010) Targeting the autophagy pathway for cancer chemoprevention. *Curr. Opin. Cell Biol.* **22**, 218-225.

Stock, M. and Otto, F. (2005) Gene deregulation in gastric cancer. *Gene* **360**, 1-19.

Tang, N.-Y., Chueh, F.-S., Yu, C.-C., Liao, C.-L., Lin, J.-J., Hsia, T.-C., Wu, K.-C., Liu, H.-C., Lu, K.-W. and Chung, J.-G. (2016) Benzyl isothiocyanate alters the gene expression with cell cycle regulation and cell death in human brain glioblastoma GBM 8401 cells. *Oncol. Rep.* **35**, 2089-2096.

Wang, F., Gómez-Sintes, R. and Boya, P. (2018) Lysosomal membrane permeabilization and cell death. *Traffic* **19**, 918-931.

Wang, Y. and Zhang, H. (2019) Regulation of autophagy by mTOR signaling pathway. *Adv. Exp. Med. Biol.* **1206**, 67-83.

Wong, V. K. W., Zeng, W., Chen, J., Yao, X. J., Leung, E. L. H., Wang, Q. Q., Chiu, P., Ko, B. C. B. and Law, B. Y. K. (2017) Tetrandrine, an activator of autophagy, induces autophagic cell death via PKC-α inhibition and mTOR-dependent mechanisms. *Front. Pharmacol.* **8**, 351.

Xiao, D., Bommareddy, A., Kim, S. H., Sehrawat, A., Hahm, E. R. and Singh, S. V. (2012) Benzyl isothiocyanate causes FoxO1-mediated autophagic death in human breast cancer cells. *PLoS ONE* **7**, e32597.

Yeh, Y. T., Hsu, Y. N., Huang, S. Y., Lin, J. S., Chen, Z. F., Chow, N. H., Su, S. H., Shyu, H. W., Lin, C. C., Huang, W. T., Yeh, H., Chih, Y. C., Huang, Y. H. and Su, S. J. (2016) Benzyl isothiocyanate promotes apoptosis of oral cancer cells via an acute redox stress-mediated DNA damage response. *Food Chem. Toxicol.* **97**, 336-345.

Yi, H., Wang, K., Du, B., He, L., Ho, H., Qiu, M., Zou, Y., Li, Q., Jin, J., Zhan, Y., Zhao, Z. and Liu, X. (2018) Aleuritolic acid impaired autophagic flux and induced apoptosis in hepatocellular carcinoma HepG2 cells. *Molecules* **23**, 1338.

Yim, W. W.-Y. and Mizushima, N. (2020) Lysosome biology in autophagy. *Cell Discov.* **6**, 6.

Yoshimori, T., Yamamoto, A., Moriyama, Y., Futai, M. and Tashiro, Y. (1991) Bafilomycin A1, a specific inhibitor of vacuolar-type H(+)-ATPase, inhibits acidification and protein degradation in lysosomes of cultured cells. *J. Biol. Chem.* **266**, 17707-17712.

Youle, R. J. and Narendra, D. P. (2011) Mechanisms of mitophagy. *Nat. Rev. Mol. Cell Biol.* **12**, 9-14.

Zhang, C., Feng, X., He, L., Zhang, Y. and Shao, L. (2020) The interrupted effect of autophagic flux and lysosomal function induced by graphene oxide in p62-dependent apoptosis of F98 cells. *J. Nanobiotechnol.* **18**, 52.

Zhang, Q. C., Pan, Z. H., Liu, B. N., Meng, Z. W., Wu, X., Zhou, Q. H. and Xu, K. (2017) Benzyl isothiocyanate induces protective autophagy in human lung cancer cells through an endoplasmic reticulum stress-mediated mechanism. *Acta Pharmacol. Sin.* **38**, 539-550.

Zhao, H., Li, Q., Pang, J., Jin, H., Li, H. and Yang, X. (2017) Blocking autophagy enhances the pro-apoptotic effect of bufalin on human gastric cancer cells through endoplasmic reticulum stress. *Biol. Open* **6**, 1416-1422.

Zhu, Y., Zhuang, J. X., Wang, Q., Zhang, H. Y. and Yang, P. (2013) Inhibitory effect of benzyl isothiocyanate on proliferation *in vitro* of human glioma cells. *Asian Pac. J. Cancer Prev.* **14**, 2607-2610.